Ordered stack of spin valves in a layered magnetoresistive perovskite

T. G. Perring

ISIS Facility, Rutherford Appleton Laboratory, Didcot, Oxon 0X11 0QX, United Kingdom

G. Aeppli

NEC Research Institute, 4 Independence Way, Princeton, New Jersey 08540

T. Kimura and Y. Tokura

Joint Research Center for Atom Technology (JRCAT), Tsukuba 305, Japan

M. A. Adams

ISIS Facility, Rutherford Appleton Laboratory, Didcot, Oxon 0X11 0QX, United Kingdom

(Received 31 August 1998)

The layered compound $La_{2-2x}Sr_{1+2x}Mn_2O_7$ ($x=0.3$) consists of bilayers of metallic MnO_2 sheets separated by insulating material. The compound exhibits markedly anisotropic magnetoresistance at temperatures well below the three-dimensional magnetic ordering temperature $T_c=90$ K in addition to colossal magnetoresistance around T_c. We present neutron-diffraction data which show that the magnetic structure of this material switches from antiferromagnetic stacking of the (ferromagnetically ordered) sheets in zero field to ferromagnetic stacking in a field of 1.5 T. To our knowledge, the data are the first to be collected on any manganite as a function of applied field, exactly as the magnetoresistance data themselves are collected. They provide a natural explanation of the low-field magnetoresistance in the ordered phase in terms of spin-polarized tunneling between the magnetic layers and suggest that the material is a bulk stack of spin-valve devices. [S0163-1829(98)52946-3]

In the past few years there has been a huge revival of interest in manganese oxides with cubic perovskite structure, $R_{1-x}A_xMnO_3$ ($R=$La, Pr, Nd and $A=$Ca, Ba, Sr, Pb), because of the very large magnetic field-induced changes in electrical resistance[1–4] they can display. The fields are typically several Tesla, however, which limits applications in technologies such as magnetic memory and sensors. One approach to increase the low-field magnetoresistance is to construct thin-film tunneling devices[5,6] where the tunnel junction provides a weak, field-sensitive link between two ferromagnetic manganites. Another possibility is to make ceramics with crystal structures consisting of multilayers of metallic MnO_2 sheets separated by insulating material. The last approach has recently succeeded with $La_{2-2x}Sr_{1+2x}Mn_2O_7$ for $x=0.3$.[7,8]

$La_{2-2x}Sr_{1+2x}Mn_2O_7$[7,8] is constructed from bilayer slices of MnO_2 sheets taken from the cubic perovskite, each slice being separated by a (La, Sr)$_2$O$_2$ spacer layer which serves to isolate the bilayers [Fig. 1(a)]. With doping of $x=0.3$ holes per Mn site the material orders magnetically below $T_c=90$ K. Above T_c the electrical resistivity [Fig. 2(a)] perpendicular to the planes follows the activated hopping law also seen for cubic material, but the in-plane resistivity remains metallic to 270 K. Below T_c the resistivity is metallic in both directions. As is common for the manganites, the magnetoresistance is greatly enhanced near T_c for currents both parallel and perpendicular to the MnO_2 planes. What is new for this bilayer material is that for temperatures far below T_c, very substantial magnetoresistance (MR) remains. Furthermore, the low-temperature MR is highly anisotropic and saturates at very small fields,[8] as Fig. 3(a) shows. The saturation field is $H_{sat}=1$ T for the samples used for Fig. 2(a) and Fig. 3(a), and is as low as 0.1 T for samples cut to minimize demagnetization.[8] The behavior for $x=0.3$ contrasts markedly with that for the more studied $x=0.4$ material. For $x=0.4$, the resistivity above and below the ordering temperature of 121 K, while very anisotropic, is qualitatively the same parallel and perpendicular to the MnO_2 planes, and the magnetoresistance in the ordered phase is both isotropic and much smaller than for the $x=0.3$ specimen.

To determine the mechanism for the magnetoresistance at $x=0.3$ we have performed magnetic neutron diffraction from single-crystal samples on the IRIS spectrometer at the pulsed neutron source ISIS in the United Kingdom. Specimens approximately 25 mm long and 4 mm in diameter with $x=0.3$ and $x=0.4$ were grown using the floating zone method. Crystals from the same batches as those used for the neutron experiments exhibited the same temperature-dependent zero-field resistivity as reported previously.[7,8] The lattice parameters at room temperature were $a=3.86$ Å, $c=20.38$ Å for $x=0.3$, and $a=3.88$ Å, $c=20.15$ Å for $x=0.4$, consistent with previously reported values.[7–9] The $x=0.4$ sample had a mosaic spread of $\sim3°$ but the $x=0.3$ sample consisted of several crystallites within a spread of $\sim8°$. Because the instrument collects data over a range of 1.5° in crystal orientation, much less than the mosaic spread, absolute intensity calibration was impossible and relative intensity comparisons are meaningful only for reflections along a ray in reciprocal space. Nevertheless, important conclusions can be drawn from the diffraction data, which for both compositions were collected in the a-c plane.

The first step was to search for temperature-dependent
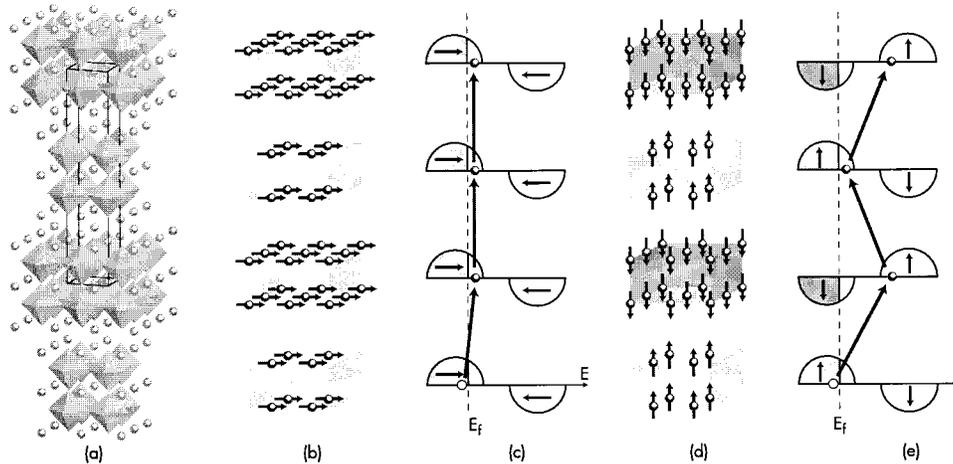
FIG. 1. (a) Structure of $La_{2-2x}Sr_{1+2x}Mn_2O_7$. The Mn ions are at the center of the MnO_6 octahedra. Circles denote La and Sr. (b) Proposed magnetic structure of the Mn sublattice for $x=0.4$ with $H=0$, and $x=0.3$ with $H=1.5T$. (c) Electronic densities of states for x and H as in (b). The conduction band contains only states with spins polarized parallel to the moments shown in (b), while the valence band is separated by a gap and is fully polarized in the opposite direction. Ordinary metallic transport (large arrows) along the c axis involves negligible energy loss and is therefore allowed. (d) Proposed magnetic structure for $x=0.3$ with $H=0$. (e) Electronic densities of states for $x=0.3$ with $H=0$. Carriers propagate along c only by tunneling across not only $(La,Sr)_2O_2$ layers but also intervening MnO_2 bilayers. The electrical resistivity associated with (d) and (e) is much higher than that associated with (b) and (c).

diffraction peaks, especially at temperatures below T_c. The only peaks found in the $(h0l)$ zone were for integer h and l. The solid circles in Figs. 2(b)–2(d) represent the temperature dependence at $H=0$ of the intensities of the (100), (004), and (005) diffraction peaks. It is apparent that lowering the temperature through T_c switches on scattering at the odd order reflections. The Bragg profiles are as sharp as those for nearby nuclear reflections, implying magnetic coherence lengths as long as those characteristic of the underlying atomic order, which we measure to be in excess of 500 Å within and perpendicular to the bilayers. Because the crystal structure is body centered tetragonal only reflections for $h+k+l$ even are expected for simple ferromagnetic order [see Fig. 1(b)]. The temperature independence of the (004) peak intensity and therefore the absence of a magnetic contribution at (004) implies that the spin orientations in a given bilayer are reversed in adjacent bilayers. The relative orientation of the spins in the two sheets that make up a bilayer can be deduced from comparing (003) and (005) intensities. Specifically, parallel alignment of nearest-neighbor spins in adjacent sheets in the bilayer modulates the $(00l)$ peak intensity as $\cos^2[\pi l/(c/a)]$, which when combined with the Mn ion magnetic form factor yields the intensity ratio $(005)/(003)$ $=18$, not far from the experimental value of 23 ± 3. In contrast, antiparallel alignment would make the ratio $(005)/(003)=0.025$.

The low-temperature and $H=0$ magnetic structure shown in Fig. 1(d) provides the simplest explanation of the neutron results given above. The coupling between different bilayers, unknown prior to this experiment, is antiferromagnetic. On the other hand, the order within the bilayers is ferromagnetic, as expected given the ferromagnetism of the similarly doped cubic perovskites $La_{1-x}Sr_xMnO_3$.[10] The moment directions in Fig. 1(d) are obtained from the low-temperature result that the $(00l)$ reflections nearly vanish (the fact that they do not do so entirely implies a small canting of the moments) and the law that neutron scattering is sensitive only to the com-

ponent of magnetic moment perpendicular to the scattering vector. The rise of the odd order $(00l)$ reflections on warming [Fig. 2(d)] implies that between 60 K and the ordering temperature, the moments rotate away from the c axis to acquire a substantial component within the sheets. Interestingly, the rapid rise in the (005) reflection, which is also accompanied by the growth of short-range magnetic correlations, sets in at the 60 K shoulder in $\rho(T)$. The main topic of the present paper, however, is the low-temperature, anisotropic magnetoresistance, which is distinct from the colossal magnetoresistance near T_c. Other phenomena, most notably polaron formation due to electron-phonon coupling, may well play the dominant role in that instance,[11] as is well documented in the cubic perovskite case.[12]

We turn now to the spin order in a magnetic field of 1.5 T, applied within the plane of the bilayers along the crystallographic b axis, that is, perpendicular to the plane in which diffraction peaks are measured. The value of 1.5 T was chosen to be sufficiently large that the resistivity perpendicular to the planes is well into the saturated regime. All odd order reflections of the form $(00l)$ disappear. Furthermore, the strong magnetic contribution at (100) found for $H=0$ immediately below T_c also disappears (the weak and largely temperature-independent diffraction found at (100) is also seen for $x=0.4$ and must arise from either a small structural distortion that breaks the tetragonal symmetry or an unknown impurity phase). The essential absence of odd order reflections implies that the magnetic moments in adjacent bilayers now point in the same direction, so that the bilayers are stacked ferromagnetically [Fig. 1(b)] rather than antiferromagnetically [Fig. 1(d)] as in zero field. That the (004) intensity, which monitors the ferromagnetism, increases monotonically as the temperature is lowered [Fig. 2(c)] means that the component of the ordered moment within the plane of the bilayers reaches a maximum at zero temperature. For $H=1.5$ T, three-dimensional order becomes clearly visible at about 125 K, rather higher than the zero-field critical
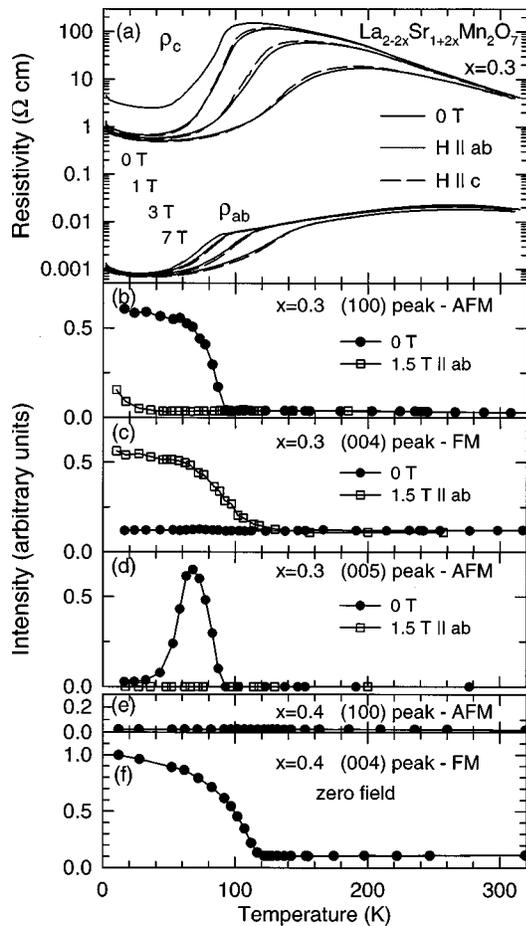
FIG. 2. Temperature dependence of (a) resistivity parallel and perpendicular to the bilayers for $x=0.3$ with various applied magnetic fields; (b)–(d) selected Bragg intensities for $x=0.3$ at zero field and 1.5 T, and (e)–(f) Bragg intensities for $x=0.4$ and zero field. Peaks with $h+k+l$ even (odd) will probe ferromagnetic (antiferromagnetic) long-range order, and are indicated by ferromagnetic (antiferromagnetic) in (b)–(f).

temperature of 90 K. A similar sized shift in the peak of the interplane resistivity in a field is also seen [Fig. 2(a)]; interpolation between the 1 and 3 T data leads to an expected shift at 1.5 T of 25 K in the resistivity maximum. This result underscores the connection between the interplane magnetic ordering and the bulk properties of $La_{2-2x}Sr_{1+2x}Mn_2O_7$, $x=0.3$.

Our proposed magnetic structure for the $x=0.3$ sample in 1.5 T is similar to the ferromagnetic order found for $x=0.4$ in zero field.[9,13,14] For example, Figs. 2(e) and 2(f) show the rise of a strong magnetic reflection at (004) but not at (100).

The discovery of coherent antiferromagnetic stacking of ferromagnetically ordered bilayers which switches to ferromagnetic stacking in a magnetic field has important consequences for the explanation of the anisotropic magnetoresistance in the ordered phase, illustrated in Figs. 1(c) and 1(e). The change in magnetic structure is accompanied by a marked reduction in the interplane resistivity but a much smaller change in the in-plane resistivity. Figure 3 shows the close correlation between the sharp switching of the resistance and the similarly sharp switching of the magnetic structure from antiferromagnetic to ferromagnetic. The figure
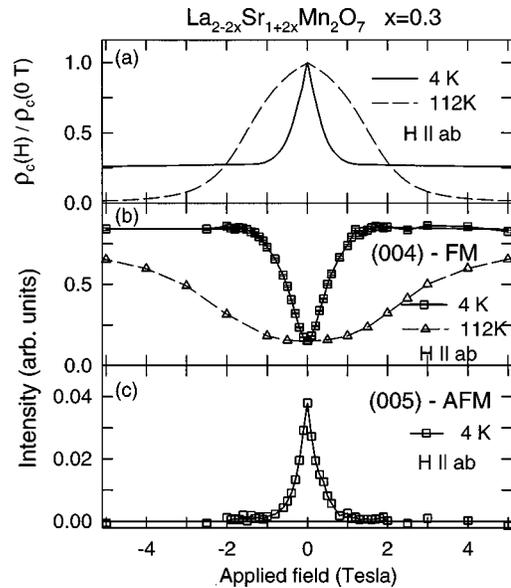
FIG. 3. (a) Field-dependent switching of resistivity, (b) ferromagnetic, and (c) antiferromagnetic Bragg intensities in the tunneling ($T=4$ K) and colossal ($T=112$ K$>T_c$) magnetoresistance regimes. We are using the very weak (005) reflection as a gauge of the antiferromagnetic stacking because in this white beam time-of-flight measurement with fixed sample and detector geometry, the portion of our wide mosaic crystal being sampled is exactly the same as for the much stronger ferromagnetic (004) reflection.

also reveals how the less field-sensitive colossal magnetoresistance correlates with the more gently field-induced ferromagnetic order near T_c. The low-temperature behavior of the resistivity is similar to that seen in artificially constructed magnetic multilayers where antiferromagnetically coupled layers of ferromagnetic iron are separated by nonferromagnetic metallic spacing layers.[15–20] An external field overwhelms the antiferromagnetic layer-to-layer coupling and so eliminates the scattering of electrons by the walls, thus reducing the resistivity. What Fig. 3 shows with directness is the analogous destruction of antiferromagnetic order in the bilayer manganite.

The dramatic features of $La_{2-2x}Sr_{1+2x}Mn_2O_7$, $x=0.3$ are that the ferromagnetic layers are (i) separated by what appear—from the c-axis resistivity above T_c—to be insulating $(La,Sr)_2O_2$ spacing layers, and (ii) are ferromagnetic metals by virtue of the double exchange mechanism. Feature (i) implies that tunneling, rather than scattering as for the giant magnetoresistance (GMR) multilayers, is likely to be at the heart of the low-temperature magnetoresistance of $La_{2-2x}Sr_{1+2x}Mn_2O_7$, $x=0.3$. Feature (ii) means that in contrast to the ferromagnetic metals in the GMR multilayers, the ferromagnetic sheets in $La_{2-2x}Sr_{1+2x}Mn_2O_7$ contain fully polarized conduction electrons in a band separated by a gap from valence bands containing only oppositely polarized states. Tunneling of electrons between adjacent sheets with the same polarizations is allowed whereas tunneling between oppositely polarized sheets is forbidden because of the need for multiple spin flips. The zero field, antiferromagnetically layered structure is therefore expected to have a much higher resistivity than the in-field, ferromagnetically layered structure. Precisely such spin-polarized transport across an insulating barrier has been observed between two thin films

(400 Å) of $La_{0.67}(Ca/Sr)_{0.33}MnO_3$ (Refs. 5 and 6) and has also been suggested as an explanation for the crystal grain-boundary-induced magnetoresistance in ceramics[21,22] and thin films[23] of the cubic perovskite manganites. As for both the individually fabricated junctions and the polycrystalline ceramics, there are also leakage currents associated with defects—most notably domain structure—in the layered manganite. These leakage currents will be shunted in parallel with the switched tunneling currents, and so will result in switching between what are ostensibly less and more metallic states. Indeed, for x just larger than 0.3 the bilayers are stacked ferromagnetically;[11] small quantities of this impurity phase could account for the shunting and also be responsible for a crystallite-dependent small temperature variation of our even order peak intensities below ~ 100 K.

In the ceramics,[21,22] the tunneling magnetoresistance is an extrinsic effect brought about by the random introduction of insulating ferromagnetic domain boundaries into the cubic perovskites. When the large low-temperature magnetoresistance was originally found for the $x = 0.3$ layered manganite, it was also attributed to random ferromagnetic domain boundaries whose probable orientation, on account of weak ferromagnetic interactions, is parallel to the MnO_2 sheets. Thus, $La_{2-2x}Sr_{1+2x}Mn_2O_7$ with $x = 0.3$ was thought to be a random stack of tunneling spin-valve devices.[8] What the sharp, field-switchable Bragg peaks in our data reveal is that this material is actually an ordered stack of such devices, and so that the large low-temperature c-axis magnetoresistance is an intrinsic effect. The measurements thus provide a concise microscopic picture of how the bilayer manganites unify the three main topics of modern research on magnetoresistance, namely the colossal magnetoresistance of the manganites, the giant magnetoresistance of intermetallic multilayers, and the tunneling magnetoresistance of thin-film devices.

[1] R. von Helmolt, J. Wecker, B. Holzapfel, L. Schulz, and K. Samwer, Phys. Rev. Lett. **71**, 2331 (1993).

[2] K. Chahara, T. Ohno, M. Kasai, and Y. Kozono, Appl. Phys. Lett. **63**, 1990 (1993).

[3] S. Jin, T. H. Tiefel, M. McCormack, R. A. Fastnacht, R. Ramesh, and L. H. Chen, Science **264**, 413 (1994).

[4] A. Urushibara, Y. Moritomo, T. Arima, A. Asamitsu, G. Gido, and Y. Tokura, Phys. Rev. B **51**, 14 103 (1995).

[5] Yu Lu, X. W. Li, G. Q. Gong, Gang Xiao, A. Gupta, P. Lecoeur, J. Z. Sun, Y. Y. Wang, and V. P. Dravid, Phys. Rev. B **54**, R8357 (1996).

[6] J. Z. Sun, W. J. Gallagher, P. R. Duncombe, L. Krusin-Elbaum, R. A. Altman, A. Gupta, Yu Lu, G. Q. Gong, and Gang Xiao, Appl. Phys. Lett. **69**, 3266 (1996).

[7] Y. Moritomo, A. Asamitsu, H. Kuwahara, and Y. Tokura, Nature (London) **380**, 141 (1996).

[8] T. Kimura, Y. Tomioka, H. Kuwahara, A. Asamitsu, M. Tamura, and Y. Tokura, Science **274**, 1698 (1996).

[9] J. F. Mitchell, D. N. Argyriou, J. D. Jorgensen, D. G. Hinks, C. D. Potter, and S. D. Bader, Phys. Rev. B **55**, 63 (1997).

[10] G. H. Jonker, Physica (Amsterdam) **22**, 707 (1956).

[11] D. Louca, G. H. Kwei, and J. F. Mitchell, Phys. Rev. Lett. **80**, 3811 (1998).

[12] A. J. Millis, Nature (London) **392**, 147 (1998).

[13] T. G. Perring, G. Aeppli, Y. Moritomo, and Y. Tokura, Phys. Rev. Lett. **78**, 3197 (1997).

[14] R. Osborn, S. Rosenkranz, D. N. Argyriou, L. Vasiliu-Doloc, J. W. Lynn, S. K. Sinha, J. F. Mitchell, K. E. Gray, and S. D. Bader, Phys. Rev. Lett. **81**, 3964 (1998).

[15] W. P. Pratt, S.-F. Lee, J. M. Slaughter, R. Loloee, P. A. Schroeder, and J. Bass, Phys. Rev. Lett. **66**, 3060 (1991).

[16] M. A. M. Gijs, S. K. J. Lenczowski, and J. B. Giesbers, Phys. Rev. Lett. **70**, 3343 (1993).

[17] A. Barthélémy, A. Fert, M. N. Baibich, S. Hadjoudj, F. Petroff, P. Etienne, R. Cabanel, S. Lequien, F. Nguyen Van Dau, and G. Creuzet, J. Appl. Phys. **67**, 5908 (1990).

[18] N. Hosoito, S. Araki, K. Mibu, and T. Shinjo, J. Phys. Soc. Jpn. **59**, 1925 (1990).

[19] S. S. P. Parkin, A. Mansour, and G. P. Felcher, Appl. Phys. Lett. **58**, 1473 (1991).

[20] J. A. Borchers and C. F. Majkrzak, in *Encyclopedia of Electronics and Electrical Engineering*, edited by J. G. Webster (Wiley & Sons, New York, in press).

[21] H. Y. Hwang, S-W. Cheong, N. P. Ong, and B. Batlogg, Phys. Rev. Lett. **77**, 2041 (1996).

[22] A. Gupta, G. Q. Gong, Gang Xiao, P. R. Duncombe, P. Lecoeur, P. Troullioud, Y. Y. Wang, V. P. Dravid, and J. Z. Sun, Phys. Rev. B **54**, R15 629 (1996).

[23] N. D. Mathur, G. Burnell, S. P. Isaac, T. J. Jackson, B.-S. Teo, J. L. MacManus-Driscoll, L. F. Cohen, J. E. Evetts, and M. G. Blamire, Nature (London) **387**, 266 (1997).